Circannual Rhythm in the Skin Gene Expression of Cashmere Goat

Jianghong Wu[1*, 3], Ying li[1], Husile Gong[2], Dubala Wu[1], Chun li[1], Bin Liu[3]

1 College of Animal Science and Technology, Inner Mongolia University for Nationalities, Tongliao, 028000, China
2 College of life science, Inner Mongolia University for Nationalities, Tongliao, 028000, China
3 Inner Mongolia Academy of Agricultural & Animal Husbandry Sciences, Hohhot, 010031, China;
* Corresponding authors: Jianghong Wu (wujianghonglong@126.com, College of Animal Science and Technology, Inner Mongolia University for Nationalities, Tongliao, 028000, China)

Abstract

The cashmere goat (*Capra hircus*) is famous for the fine quality cashmere wool. The cashmere is produced by secondary hair follicle that the growth shows seasonal rhythm. Thus, in this study, the skin of cashmere goat was selected as a model to illustrate the circannual rhythm of skin. The whole length skin transcriptome mixed from selected four months was obtained by PacBio single-molecule long-read sequencing (SMRT) technology. We generated 82,382 high quality non-redundant transcripts belonging to 193,310 genes, including 4,237 novel genes. Other 39 skin transcriptomes sampled from Dec. 2014 to Dec. 2015 were sequenced by Illumina Hi-Seq2500, we found 980 genes were differentially expressed. Of these genes, 403 seasonal rhythm genes (SRGs) were expressed and exhibited a seasonal pattern in skin. The results also showed that miRNAs were differentially expressed as the daylight length changed throughout a year. Some SRG genes related to the hormone secretion and eyes morphogenesis were enriched in skin. These genes gradually increased their expression level under short light, reached the peak near the summer solstice, and then began to decline. We found that the expression of Dio1 gene may be affected by the photoperiod that induces transformation from the inactive T4 to active thyroid hormone T3 in the skin and led to the difference between the skin circannual rhythm and the core circannual rhythm. Furthermore, the skin expressed eye morphogenesis-related genes and miRNAs, which suggested some cells in the skin could have the potential of light sensitivity. These results revealed that SRGs could regulate the downstream gene expression and physiological process in the skin to adapt to the season change.

Keywords: Circannual Rhythm, Cashmere Goat Skin, Thyroid Hormone, Seasonal Rhythm Genes, PacBio SMRT Sequencing

Introduction

To survive and reproduce, all living organisms must adapt to environmental variation. The thousands of genes of human blood have seasonal expression profiles, with inverted patterns observed between Northern and Southern hemispheres[1]. Thus, the gene expression of organisms would be regulated by the factors of the environment. Among these factors, the photoperiod is the most important clue for animals to adjusting the physiological state to the circadian and circannual rhythms that resulted from rotation and revolution of earth.

Although the eye is very important in the formation of rhythms, the skin is the largest tissue of

the organism, which has the functions of defense, protection, and perception (such as the perception of seasonal changes). In the long evolution of living things, skin adapts to different habitats (water to land to sky, wet to dry, hot to cold) and evolves different types of skin. When multicellular organisms evolved to Annelida, they still didn't have eyes. Before the appearance of special photosensitive organs, the skin had played a role in sensing the external environment (light). Light can directly affect the cell growth cycle[2], and light can directly regulate the expression of a biological clock gene per in cells [3]. Further studies have found that the phenomenon of the direct control of circadian clock by light without SCN is common in fish [4, 5]. Miki Tanioka et al. first found fluctuating biomolecular clocks in the skin of mice[6]. However, subsequent studies found that both rat dermal fibroblasts [7] and human keratinocytes cultured in vitro have the same rhythm as the peripheral biological clock, and the external environment (drugs, serum) can affect the biological clock of cells cultured in vitro[8-10]. The circadian clocks of individual cells cultured in vitro are controlled by themselves, and the circadian clocks can be transmitted to the progeny cells through the process of cell division and proliferation[11]. Different types of cells in the skin have different biological clock phases. The final biological clock in the skin is formed by the coordination of various types of cell biological clock genes[12]. Therefore, the biological clock in the skin is very complex and has memory potential, which is easily affected by light.

The economic performance of livestock is mostly related to seasonal rhythm, especially the animals living in the temperate zone. In order to synchronously change physiological conditions and phenotypic behavior with environmental conditions, animals need to rely on environmental cues to judge the coming season. It is generally believed that mammals perceive the light and darkness of the outside world through the retina, and transmit the photoperiod messages to the hypothalamus through the content of melatonin in the pineal gland which depends on light to control the physiological rhythm so that the biological clock in the body keeps the same rhythm with the environment. The circannual rhythms are essential for animal production. Therefore, the study on the mechanism of how livestock adjusts gene expression in different tissues to adapt the biological systems to change physiological behavior with seasonal changes can provide a theoretical basis for animal husbandry production.

Results

Skin transcriptome of cashmere goat skin

To obtain a representative whole length transcriptome of skin, we collected body side skin and ear skin from three Inner Mongolia Cashmere Goats at four time points (Jan, Apr, Jul, Oct) and employed PacBio single-molecule long-read sequencing (SMRT) technology. 591,585 circular consensus (CCS) reads were obtained. Of the total reads, 466,058 (78.78%) were full length reads non-chimeric (FLNC) sequences were identified. After Iterative Clustering, 149,604 consensus isoforms were polished and 137,211 high quality FLNC transcripts were classified, with the criteria post-correction accuracy above 99%. The high-quality Illumina sequences were used to improve the quality of long reads. Finally, 82,382 high quality and non-redundant transcripts were obtained, which belongs to 18,919 genes, including 4,237 novel genes.

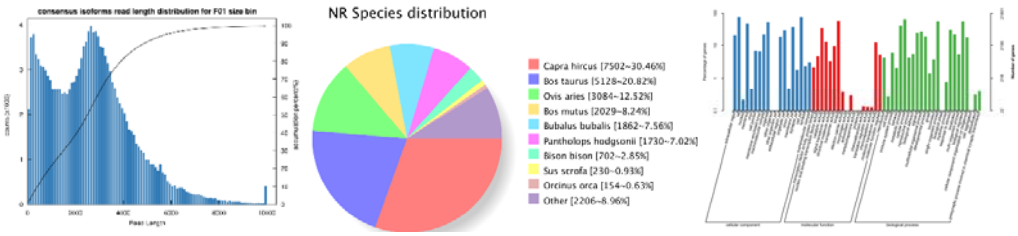

Figure 1 Summary of PacBio RS II SMRT sequencing of *cashmere goat skin* transcripts. **(a)** consensus isoforms read length distribution, **(b)** the species distribution of gene annotation based the NR database, **(c)** GO annotation, where blue represents a cellular component, red represents a molecular function, and the green represents a biological process.

To reveal Annual Rhythm under natural conditions, we chose Cashmere goats, strict seasonal molt livestock as the study species. Skin samples were collected at noon every month for one year, from December 2014 to December 2015, from the bodyside of three natural goats. In total, transcriptomes of 39 skin samples were obtained by Illumina sequencing (RNA-Seq). After the reads filtering, clean data were obtained. To calculate the expression level of skin genes, salmon[13] software was utilized based on the whole length transcriptome reference sequence. Finally, 980 genes were significantly differential expression in goat skin among the different month. The sample correlation matrix showed that the transcriptomes of goat skin were divided long daylight (April, May, Jun, July, August) and short daylight group (September, October, November, December, January, February, March) (Figure 2). This result suggested that these DEGs could be expressed in the skin under the certain rhythm.

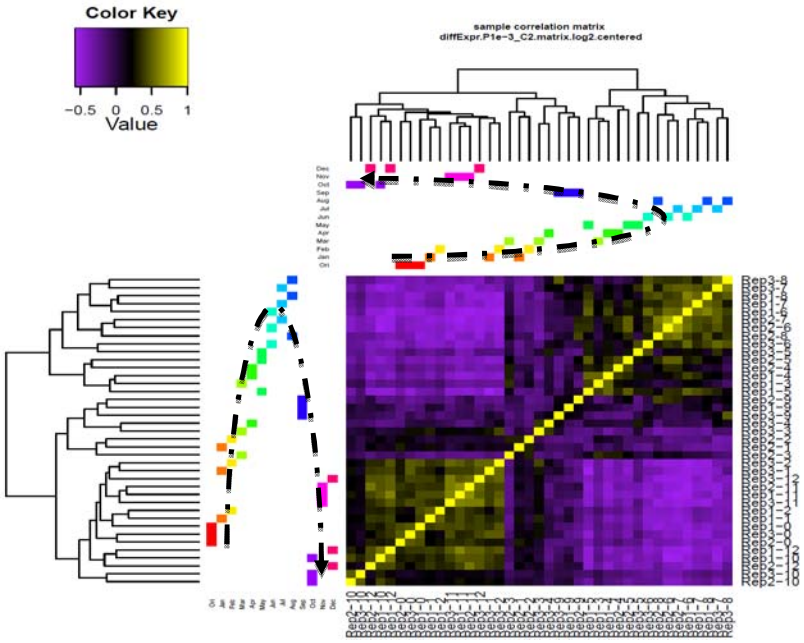

Figure2 sample correlation matrix based the skin transcriptomes

To understand the dynamics of chromosome expression, we analyzed the distribution of DEGs on each chromosome and calculated the density of DEGs. The results showed that the genes on the Chr1 and Chr19 were significantly activated. Furthermore, we found the KP and KAP tandem region on those two chromosomes (figure 3).

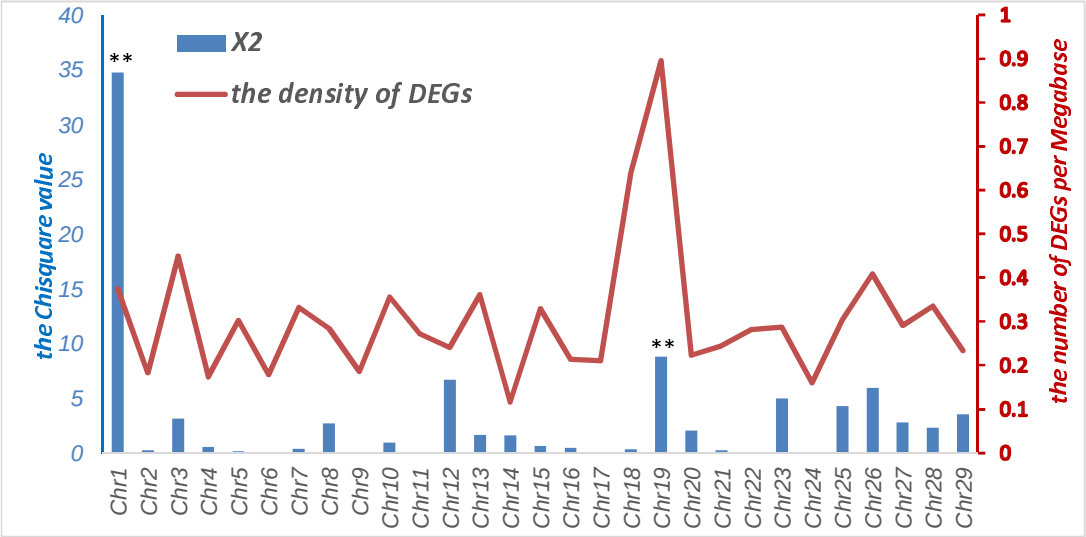

Figure 3 the distribution of DEGs on the chromosome

Annual Rhythm Expressed Genes in Goat Skin

To analyze the rhythm of DEGs of goat skin, MetaCycle was utilized. We tried from 4 months to one year as a length of interesting rhythms. Finally, 403 genes of those DEGs expressed in the skin as circannual rhythm (Figure 4), which divided two groups long daylight genes and short daylight genes.

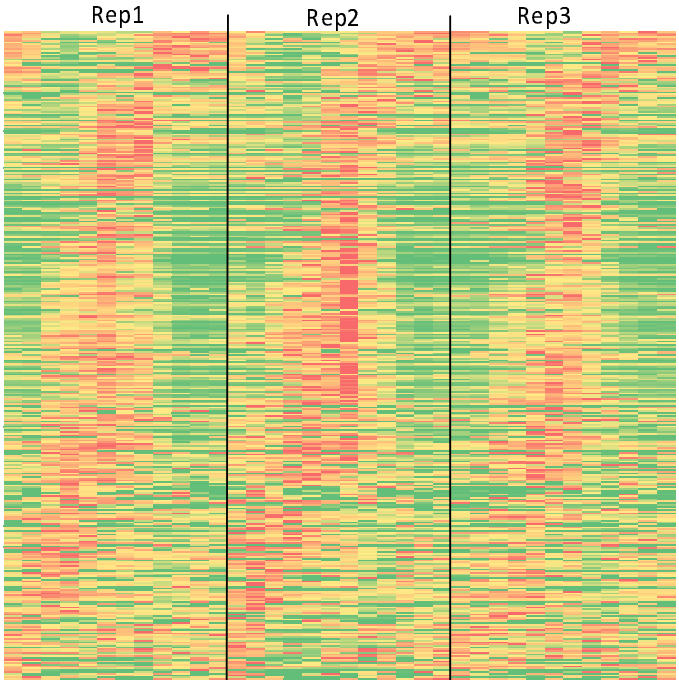

Figure 4. the heat map of the seasonal rhythm genes in cashmere goat skin

We found that 90 transcript factors (TFs) and 76 TF cofactors (Supplement file 1) in these seasonal rhythm genes (SRGs) of goat skin based on the AnimalTFDB [14]. Of these SRGs, 18 ncRNAs were highly expressed in skin. And results also showed that there are 28 genes related to secretoglobin family and the S100 family with highly expression (Table 1). Furthermore, to infer the potential up stream regulators of SRGs, we investigated the transcript binding site on the 5' UTR of SRGs. Many of the ZNF motif and the KLF motif located in the FCR of SRGs (Supplement file 1). KLF family members have related to the pathways of BMAL1-CLOCK and NPAS2, which could activate circadian gene expression and Adipogenesis.

Table 1 The genes related with secretoglobin family and the S100 family

RefSeq Accession Number	Gene symbols	Gene description	Maximum expression value (RPKM)
XM_005692259.2	LOC102169125	major allergen I polypeptide chain 2	45989.907
XM_018062299.1	LOC106503120	major allergen I polypeptide chain 1	45277.958
XM_005692256.2	LOC102191166	major allergen I polypeptide chain 1-like	40423.136
XM_013971277.2	LOC102191453	secretoglobin family 2B member 2-like	32363.733
XM_018062302.1	LOC108637981	major allergen I polypeptide chain 1-like	31126.557
XM_018044050.1	LOC102188300	odorant-binding protein	11397.749
XM_005692260.3	LOC102169411	major allergen I polypeptide chain 1-like	10994.02
XM_018044026.1	LOC102186944	allergen Bos d 2	9852.28
XM_005692261.2	LOC102169695	major allergen I polypeptide chain 2	9054.857
XM_005677509.2	LOC108633164	protein S100-A7-like	7418.243
XM_005701239.2	LOC102189201	allergen Bos d 2	6038.088
XM_005677510.2	LOC108633164	protein S100-A7-like	3554.848
XM_018046586.1	S100A7A	protein S100-A7A	2872.84
XR_001919671.1	LOC102180344		2441.43
XM_005692255.2	LOC102190903	androgen-binding protein homolog	2432.44
XM_018046587.1	S100A7A	protein S100-A7A	2122.853
XM_018044027.1	LOC102186944	allergen Bos d 2	2112.612
XM_005677513.3	S100A8	protein S100-A8	1697.389
XR_311282.2	LOC102187389		1392.066
XM_018046133.1	LOC102169149	protein S100-A12	1185.225
XM_013977249.2	S100A9	protein S100-A9	566.149
NM_001285548.1	LTF	lactotransferrin precursor	312.126
XM_018065147.1	LOC102182869	primary amine oxidase, lung isozyme-like isoform X1	299.292
XR_310700.1	LOC102191729		270.069
XM_018062304.1	LOC102168852	major allergen I polypeptide chain 1-like	247.89

XM_018046132.1	S100A9	protein S100-A9	81.69
XM_005679934.3	KRT4	keratin, type II cytoskeletal 4	64.26
XM_005693167.3	LOC102179878	WAP four-disulfide core domain protein 18	62.968

The molecular basis of hair growth

To character the hair cycle on the molecular level, we chosen keratin protein (KP) genes and keratin-associated protein (KAP) genes from the DEGs, which are the majority of cashmere composition. In this study, of those DEGs, 55 genes of KP and KAP were found and highly expressed in goat skin during the changing of the season. There are 37 transcripts that reached the peak of expression level at August and highly expressed during June to September, which was earlier than the hair follicle activity (figure 5). The majority of these genes are located on the Chr1:141.4M-144.5M and Chr19:41.0M-41.3M, which according to the chromosomal distribution of DEGs.

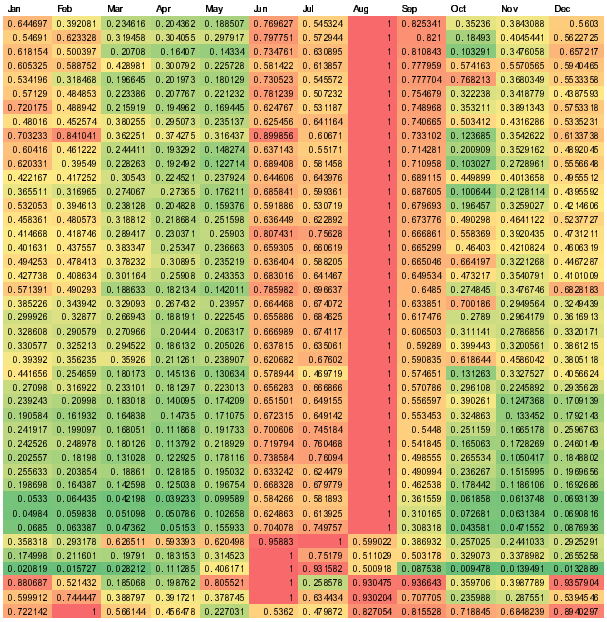

Jan	Feb	Mar	Apr	May	Jun	Jul	Aug	Sep	Oct	Nov	Dec	
0.644697	0.392081	0.234616	0.204362	0.188507	0.769627	0.545324	1	0.825341	0.35236	0.3843088	0.5603	keratin-associated protein 9-2-like
0.54691	0.623328	0.319458	0.304055	0.297917	0.797751	0.572944	1	0.821	0.18493	0.4045441	0.5622725	keratin-associated protein 4-9-like isoform X1
0.618154	0.500397	0.20708	0.16407	0.14334	0.734761	0.630895	1	0.810843	0.103291	0.3476058	0.657217	keratin-associated protein 9-9-like
0.605325	0.588752	0.428981	0.300792	0.225728	0.581422	0.613857	1	0.777959	0.574163	0.5570565	0.5940465	keratin-associated protein 17-1
0.534196	0.318468	0.196645	0.201973	0.180129	0.730523	0.545572	1	0.777704	0.768213	0.3680349	0.5533358	keratin-associated protein 9-9-like
0.57129	0.484853	0.223386	0.207767	0.221232	0.781239	0.507232	1	0.754679	0.322238	0.3418779	0.4875593	keratin-associated protein 4-9
0.720175	0.488942	0.215919	0.194962	0.169445	0.624767	0.531187	1	0.748968	0.353211	0.3891343	0.5753318	keratin-associated protein 9-9-like
0.48016	0.452574	0.380255	0.295073	0.235137	0.625456	0.641164	1	0.740665	0.503412	0.4316286	0.5335231	keratin, ultra high-sulfur matrix protein isoform X1
0.703233	0.841041	0.362251	0.374275	0.316437	0.899856	0.60671	1	0.733102	0.123685	0.3542622	0.6133738	keratin-associated protein 4-9-like
0.60416	0.461222	0.244411	0.193292	0.148274	0.637143	0.55171	1	0.714281	0.200909	0.3529162	0.4892045	keratin-associated protein 9-2-like
0.620331	0.39549	0.228263	0.192492	0.122714	0.689408	0.581458	1	0.710958	0.103027	0.2728961	0.5556646	keratin-associated protein 9-2-like
0.422167	0.417252	0.30543	0.224521	0.237924	0.644606	0.643976	1	0.689115	0.449899	0.4013658	0.4955512	keratin-associated protein 12-2-like
0.365511	0.316965	0.274067	0.27365	0.176211	0.685841	0.599361	1	0.687605	0.100644	0.2128114	0.4395592	keratin-associated protein 10-7-like isoform X1
0.532053	0.394613	0.238128	0.204828	0.159376	0.591886	0.530719	1	0.679693	0.196457	0.3259027	0.4214606	keratin-associated protein 9-2-like
0.458361	0.480573	0.318812	0.218684	0.251598	0.636449	0.622892	1	0.673776	0.490298	0.4641122	0.5237727	keratin-associated protein 12-2-like
0.414668	0.418746	0.289417	0.230371	0.25903	0.807431	0.75628	1	0.666861	0.558369	0.3920435	0.4731211	keratin associated protein 3.1
0.401631	0.437557	0.383347	0.25347	0.236663	0.659305	0.660619	1	0.665299	0.46403	0.4210824	0.4606319	keratin-associated protein 10-12-like
0.494253	0.478413	0.376232	0.30895	0.235219	0.636404	0.586205	1	0.665046	0.664197	0.3221268	0.4467287	keratin, ultra high-sulfur matrix protein isoform X1
0.427738	0.408634	0.301164	0.25908	0.243353	0.683016	0.641467	1	0.649534	0.473217	0.3540791	0.4101009	keratin associated protein 12.1
0.571391	0.490293	0.188633	0.182134	0.142011	0.785982	0.696637	1	0.6485	0.274845	0.3476746	0.6628183	keratin-associated protein 9-2
0.385226	0.343942	0.329093	0.267432	0.23957	0.664468	0.674072	1	0.633851	0.700186	0.2949564	0.3249439	keratin-associated protein 12-2
0.299926	0.32877	0.266943	0.188191	0.222545	0.655886	0.684625	1	0.617476	0.2789	0.2964179	0.3616913	keratin-associated protein 10-8
0.328608	0.290579	0.270966	0.20444	0.206317	0.666989	0.674117	1	0.606503	0.311141	0.2786856	0.3320171	keratin-associated protein 10-8-like
0.330577	0.325213	0.294522	0.186132	0.205026	0.637815	0.635061	1	0.59289	0.399443	0.3200561	0.3861215	keratin-associated protein 10-12-like
0.39392	0.356235	0.35926	0.211261	0.238907	0.620682	0.67602	1	0.590835	0.618644	0.4566042	0.3805118	keratin-associated protein 10-7-like isoform X1
0.441656	0.254659	0.180173	0.145136	0.130634	0.578944	0.469719	1	0.574651	0.131263	0.3327527	0.4056624	keratin-associated protein 9-8-like
0.27098	0.316922	0.233101	0.181297	0.223013	0.656283	0.666866	1	0.570786	0.296108	0.2245892	0.2935628	keratin-associated protein 10-8-like
0.239243	0.20998	0.183018	0.140095	0.174209	0.651501	0.649155	1	0.556597	0.390261	0.1247368	0.1709139	keratin-associated protein 10-11-like
0.190584	0.161932	0.164838	0.14735	0.171075	0.672315	0.649142	1	0.553453	0.324863	0.133452	0.1792143	keratin-associated protein 10-8-like
0.241917	0.199097	0.168051	0.111868	0.191733	0.700606	0.745184	1	0.5448	0.251159	0.1665178	0.2596763	keratin-associated protein 10-8-like
0.242526	0.248978	0.180126	0.113792	0.218929	0.719794	0.760468	1	0.541845	0.165063	0.1728269	0.2460149	keratin-associated protein 10-1 isoform X1
0.202557	0.18198	0.131028	0.122925	0.178116	0.738584	0.76094	1	0.498555	0.265534	0.1050417	0.1848602	keratin-associated protein 10-8-like
0.255633	0.203854	0.18861	0.128185	0.195032	0.633242	0.624479	1	0.490994	0.236267	0.1515995	0.1989656	keratin-associated protein 10-8-like
0.198698	0.164387	0.142598	0.125038	0.196754	0.668328	0.679779	1	0.462538	0.178442	0.1186106	0.1692686	keratin-associated protein 10-8-like
0.0533	0.064435	0.042198	0.039233	0.099589	0.584266	0.581893	1	0.361559	0.061858	0.0613748	0.0693139	keratin, type I cuticular Ha8
0.04984	0.059838	0.051098	0.050786	0.102658	0.624863	0.613925	1	0.310165	0.072681	0.0631384	0.0690816	keratin, type I cuticular Ha7-like
0.0685	0.063387	0.047362	0.05153	0.155933	0.704078	0.749757	1	0.308318	0.043581	0.0471552	0.0676936	keratin-associated protein 10-9-like
0.358318	0.293178	0.626511	0.593393	0.620498	0.95883	1	0.599022	0.386932	0.257025	0.2441033	0.2925291	keratin, type I cytoskeletal 18
0.174998	0.211601	0.19791	0.183153	0.314523	1	0.75179	0.511029	0.503178	0.329073	0.3378982	0.2655258	keratin, type II cytoskeletal 6A-like
0.020819	0.015727	0.028212	0.111285	0.406171	1	0.931582	0.500918	0.087538	0.009478	0.0139491	0.0132889	keratin, type II cytoskeletal 4
0.880687	0.521432	0.185068	0.198762	0.805521	1	0.258578	0.930475	0.936643	0.359706	0.3987789	0.9357904	keratin-associated protein 4-9-like isoform X3
0.599912	0.744447	0.388797	0.391721	0.378745	1	0.634434	0.930204	0.707705	0.235988	0.287551	0.5394546	keratin-associated protein 4-8-like
0.722142	1	0.566144	0.456478	0.227031	0.5362	0.479872	0.827054	0.815528	0.718845	0.6848239	0.8940297	keratin, high-sulfur matrix protein, B2D-like

Figure 5 the expression matrix of the keratin protein genes and keratin-associated protein genes in skin at one year.

The function enrichment of seasonal rhythm genes

The function of seasonal rhythm genes in the skin was enriched by the ClueGO, and eighteen clusters GO terms were classified. Most of the GO terms involved in the biological process of organ growth and development, signal transduction, response stimulate from activity components (Figure 6A). Of these GO clusters, eye morphogenesis and camera-type eye morphogenesis were enrichment in cashmere goat skin. Therefore, we interest in whether the skin also has the sensor for light. To deeply analyze the expression pattern of eye morphogenesis genes, we drew the expression value of those genes related to the processes. The majority of these genes were highly expressed in the skin during in long daylight of year (Figure 6B).

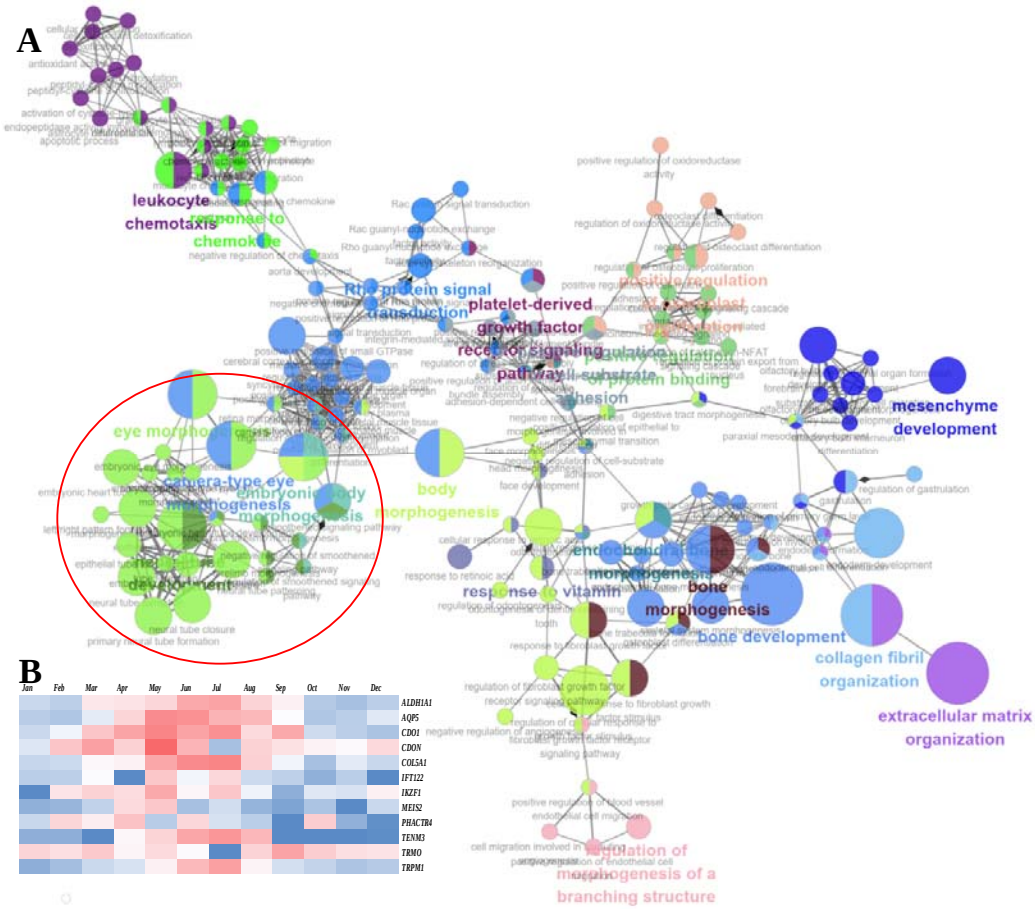

Figure 6. the Function Enrichment and Expression Pattern. **A,** the Function Enrichment for Annual Rhythm Expressed Genes based on the GO (biological process), the red circle showed that those biological process related with the development of eye. **B**, the expression pattern of eye morphogenesis genes.

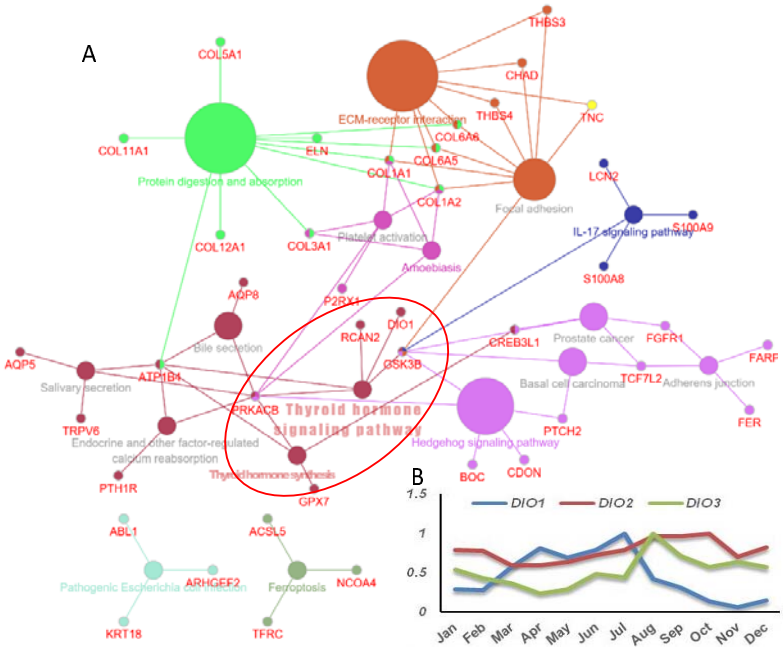

Figure 7 the Function Enrichment for Annual Rhythm Expressed Genes based on the KEGG, the red circle showed that thyroid hormone pathway and genes.

The thyroid hormone signaling pathway and thyroid hormone synthesis were enriched by ClueGO (figure 7A). Three types deiodinase, DIO1, DIO2, and DIO3, were expressed in the skin of cashmere goats (figure 7B), which was essential to the regulation of thyroid hormone activity. To deeply analyze the expression pattern of thyroid hormone related genes, we drew the expression value of those genes related to the processes. The expressed trend of these genes was showed a certain rhythmic pattern in the skin during the whole year (figure 8).

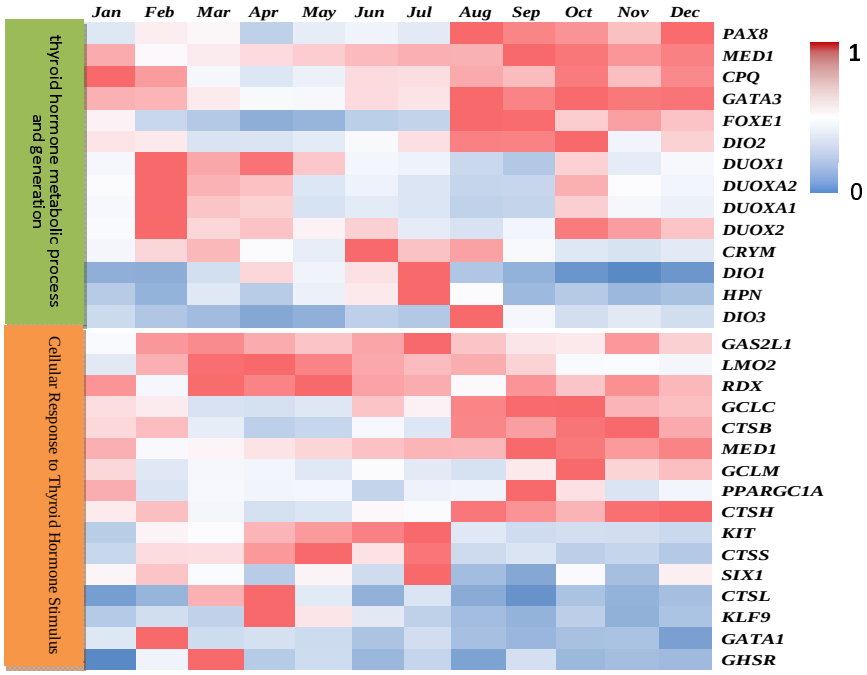

Figure 8 the expression pattern of thyroid hormone associate genes.

The differential expressed miRNA in goat skin during seasonal variation

To investigate whether the miRNA would variate during seasonal changed, we also used NGS to sequence the miRNA in cashmere goat skin. 1973 mature miRNAs were predicted based on the miRDeep2 software, which contains 436 known goat mature miRNAs and 1537 novel miRNAs. 35 miRNAs were differentially expressed between winter and summer, which was the biggest difference among four seasons (table 2). Of these differential expressed miRNAs (DEMs), 33 miRNAs were up and 2 were down-regulated in winter, compared to summer (Supplement file 2). The chi-miR-206 was highly expressed in winter compared with the summer which indicated that miR-206 is also an important regulator of the circannual rhythm excepting an important regulator of the circadian clock[15]. Chi-miR-211 and chi-miR-144 expressed lower in winter compared with the summer.

Table 2 the number of DEMs among different seasons

	Spring	Summer	Fall	Winter
Spring	0	0	0	0
Summer	0	0	2	35
Fall	0	2	0	2
Winter	0	35	2	0

The expression trend of DEMs was opposite with the SRGs in skin during the seasonal variation. To integrate the miRNA and SRGs, we utilized the Mirnada to detect the potential binding sites. Of those SRGs, 151 genes have the interaction with 35 miRNAs based on the Mirnada. Then, the interaction networks were visualized in Cytoscape, which constructed from 186 genes (nodes) and 998 interactions (edges) (Figure 9).

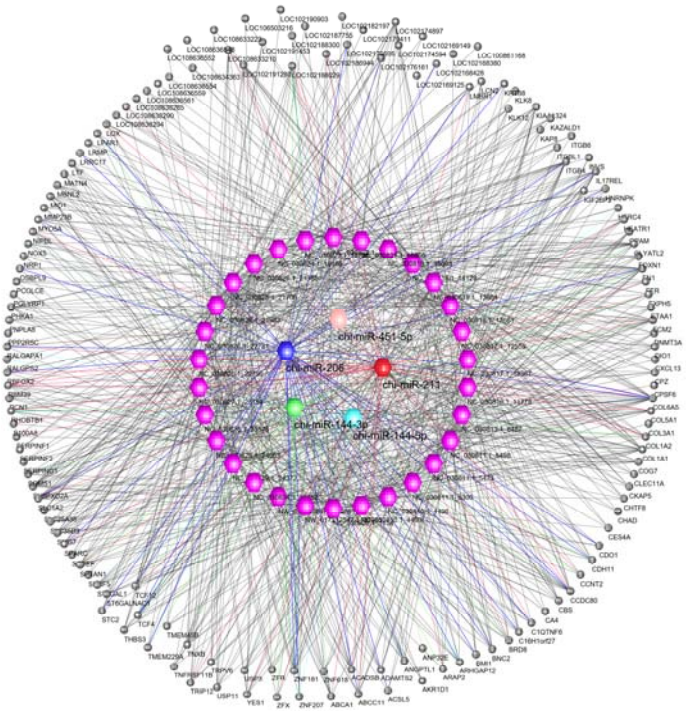

Figure 9 the interaction networks between seasonal rhythmal genes and differential expressed miRNAs during seasonal variation. Inner cycle for miRNA and outer cycle for SRGs. The purple miRNAs were novel miRNAs based on the miRDeep2.

Discussion

In this study, 403 seasonal rhythm genes were obtained by analyzing the dynamic transcriptome of cashmere goat skin. However, the classic circadian clock genes (ClOCK, BMAL1, PER, TIM, CRY, CSNK)[16] did not show significant seasonal changes in cashmere goat skin. The results suggested that there might be differences in gene sets controlling seasonal rhythm and circadian rhythm. However, many KLF motifs located in the FCR of SRGs, which indicated that the regulation of the circannual rhythm in skin could depends the circadian clock.

Through the functional classification of 403 seasonal rhythm genes (SRGs), it is found that these genes are involved in the synthesis of various hormones (thyroid hormones), sensory organ

development (eyes), keratinocyte differentiation (such as epidermal differentiation complex gene cluster gene) and other functions. It is generally believed that seasonal rhythms consist of complex transcription and translation feedback pathways, which activate specific transcription factors through thyroid hormones. The results showed that the coding genes of type I deiodinase (DIO1) was expressed in the skin of cashmere goats as seasonal rhythm. The expression of DIO1 gene in cashmere goat skin increased gradually under short light but decreased gradually under long light. In addition to the ability to deionize T4 and transform it into T3, DIO1 can also remove the excessive thyroid hormone T4 in the tissue and protect the body from the damage caused by hyperthyroidism[17, 18]. The skin and hair follicle express almost all thyroxine receptor proteins[19-21], which shows that the skin can make precise regulation on seasonal thyroid hormones to adapt to seasonal changes and regulate the expression of transcripts in cells to achieve physiological behavior feedback of organisms. The expression of Dio1 in cashmere goat skin increased gradually under short light, reached the peak before and after the summer solstice, and then began to decline, which was equivalent to increasing the concentration of T3 in cashmere goat skin in autumn and winter. With the increase of T3 concentration in autumn and winter, the activity of secondary hair follicle stem cells increased, and then the growth of villi started.

CHGA gene belongs to the short light labeling of thyrotropin cells, and the long light thyrotropin cells labeled by the EYA3 gene maintain the annual biological rhythm of pituitary nodule through the transformation of two-phase state[22]. In this study, CHGA was expressed in the skin of cashmere goats as seasonal rhythm keeping step with the Dio1 gene. Although the expression of CHGA in the skin of cashmere goat is not consistent with that in the pituitary nodule, the regulation of seasonal rhythm in the skin may be different from that in the brain. Of the SRGs, those genes related to the eye morphogenesis were enriched, such as AQP5 and TRPM1. Both of them are highly expressed during long daylight. AQPs play important roles in all ocular tissues and involved in the eyes morphogenesis[23]. Mutations in TRPM1 (Transient Receptor Potential Cation Channel Subfamily M Member 1) could induce complete congenital stationary night blindness[24]. UVB could affect the activity of the p53□TRPM1/miR□211□MMP9 axis in human melanocyte and induce melanocyte migration [25]. In this study, we also found that chi-miR-211 was highly expressed in cashmere goat skin in summer. MiR-211 is essential for adult cone photoreceptor maintenance[26]. These results suggested that some cells in the skin could have the potential of photosensitive, which could maintain the specific rhythm of the peripheral organs based on the environment factor (photoperiod).

The results also showed that the epidermal differentiation complex (EDC) genes gradually increase under short light, reaches the peak at about the summer solstice, and then the expression amount begins to decline. The main function of EDC is to drive keratinocyte differentiation and promote epidermal and hair follicle differentiation, which may be the reason why cashmere goats began to grow cashmere at the end of June and the beginning of July. Among them, S100A7, S100A8, S100A9 and S100A12 genes are all innate immune regulatory elements [27] in humans, indicating that skin plays an important role in organism protection and environmental perception. The level of S100A7 expressed in human normal skin is very low, and only under pathological conditions (such as melanoma) will the expression increase[14, 28-30]. This may suggest that S100 gene family members or EDC gene cluster members of cashmere goats have different biological functions from humans and mice. The S100A7 of ungulates has accelerated evolution[31], thus S100A7 gene of cashmere goat may have evolved different functions from

human and mouse. Furthermore, the S100A7 gene can be induced and expressed by ultraviolet light in vitro and in vivo, with a dose-dependent effect[32]. Ultraviolet radiation and retinoic acid both can stimulate normal keratinocytes to secrete S100A7 protein, and finally inhibit the differentiation of keratinocytes[33].

The expression pattern of S100A7 in the skin of cashmere goats was highly correlated with the changing trend of UV intensity in the growing place[31]. It has also been reported that S100A7 can regulate β-catenin signaling pathway[34], while Wnt signal cannot induce the expression of S100 family protein[35], which is unidirectional. Therefore, UV may induce the differentiation and development of skin and hair follicle by affecting the expression of specific genes in the skin of cashmere goat, and then form the seasonal growth of villi. However, the accumulation of β-Catenin is very important for the activation and proliferation of hair follicle stem cells. When the thyroid hormone receptor (TR) is knocked out, the proliferation of hair and epidermis in mice is limited[36], and the expression of several miRNAs related to skin homeostasis is significantly reduced[37]. The expression of S100A8 and S100A9 in the skin of knockout mice treated with retinoic acid increased significantly[38], indicating that TRs receptor related pathways may be related to the regulation of S100 expression. Further, it was found that T3 could increase S100 expression in Schwann cells[39], which indicated that T3 could regulate the epidermal differentiation complex genes such as S100, and then regulate the activity of Wnt and other hair follicle development related signal pathways.

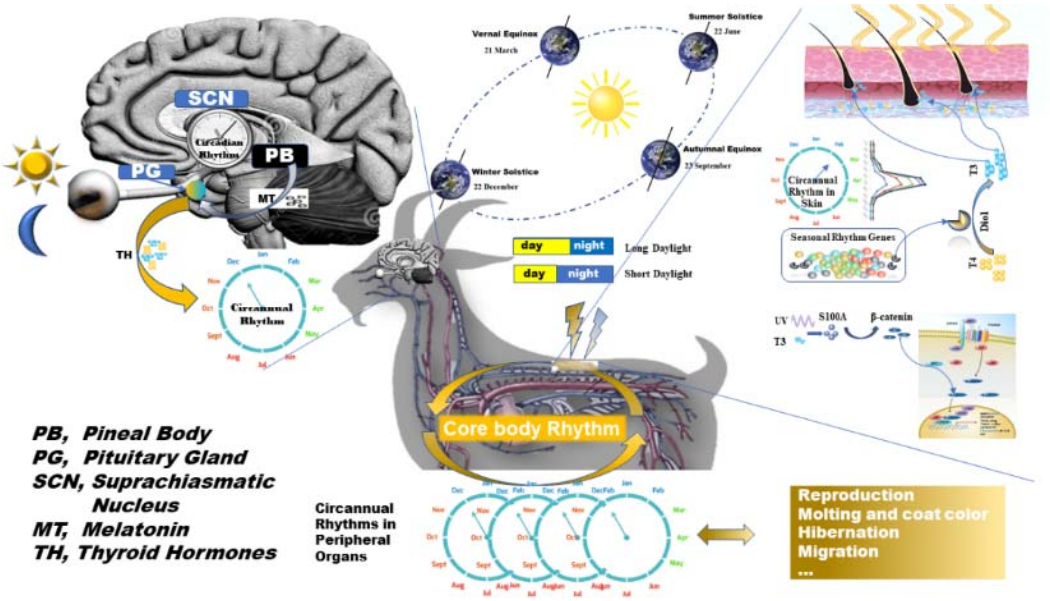

Figure 10 the Hypothesis of the Skin Circannual Rhythm Interaction with the Photoperiod

Taking together, we provided a hypothesis to describe that the goat skin how to make the own rhythm and get the clue from the environment factor. The melatonin, produced by the pineal body, dependent upon the transmission of the light through the eye, which decided the circadian rhythm. While melatonin could inhibit the activity of the thyroid gland through the pituitary gland and decrease the secretion of thyroid hormone. Then the content of thyroid hormone in blood circulation maintains the core body circannual rhythm of a goat. When the compounds of TH, T3

and T4, reached to the peripheral organs such as skin, the located deiodinase regulating the transformation from the T4 to T3. The expression level of deiodinase or other molecules affected by the environment factor such as the photoperiod. Finally, the interaction of transcript factor in SRGs and miRNAs regulated the gene expression profile and psychological process in the skin to adjust the season change. However, it needs more advanced functional experiments in the future to identify the details of how the skin gene expression profile adjusts to season variation.

Method and Materials

Experimental animals and the location.

Cashmere goat is a famous livestock species for the cashmere. We collected skin samples of body side from three Inner Mongolia Cashmere Goats. As the experimental goats were located at Tumed Zuoqi, Huhhot, China (N40°30′22.89″E110°54′47.29), the time series UV index at 40 degrees north latitude proximity (from Dec 1, 2014 to Dec 31, 2015) were downloaded from the Tropospheric Emission Monitoring Internet Service (http://www.temis.nl/index.php). We collected skin samples up to ~1.5 cm^2 seasonal and the samples were immediately stored at liquid nitrogen before RNA extraction. Samples for the seasonal experiment were collected from 1 January 2014 to 1 December 2014 on the Tumed Zuoqi (sample ID 1–36).

SMRT sequencing of full-length transcriptome of skin

We collected body side skin and ear skin from three Inner Mongolia Cashmere Goats at four time points (Jan, Apr, Jul, Oct). The RNA samples were extracted with Trizol from skin sample. Equal amounts of total RNA from each skin sample were pooled prior to library construction. The SMART sequencing library was constructed according to the Iso-Seq protocol. Full-length cDNAs of mRNAs were synthesized by SMARTer™ PCR cDNA Synthesis Kit. PacBio Iso-Seq libraries were prepared following the PacBio Standard Library prep protocol. Sequencing was performed on a PacBio RsII instrument. Both TGS, SGS and sRNA was performed by Biomarker Technology Co. (Beijing, China).

Raw reads were processed into error corrected reads of insert (ROIs) using Iso-seq pipeline with minFullPass=3 and minPredictedAccuracy=0.9. Next, full-length, non-chemiric (FLNC) transcripts were determined by searching for the polyA tail signal and the 5’ and 3’ cDNA primers in ROIs. ICE (Iterative Clustering for Error Correction) was used to obtain consensus isoforms and FL consensus sequences from ICE was polished using Quiver. High quality FL transcripts were classified with the criteria post-correction accuracy above 99%. FL consensus sequences were mapped to reference genome using GMAP. Mapped reads were further collapsed by pbtranscript-ToFU package with min-coverage=85% and min-identity=90%. 5’ difference was not considered when collapsing redundant transcripts.

Annual Transcriptome of Cashmere Goat Skin

Total RNA was extracted using a RNeasy Mini Kit (Qiagen) from a skin sample. The amount of RNA was measured using a Nanodrop or Qubit 2.0 (Thermo Fisher Scientific), and the quality was assessed using an Aglient 2100 (Agilent Technologies). The RNA-seq library was constructed with 150bp paired-end sequences for each sample, according to the standard protocol provided by Illumina, Inc. (San Diego, CA, USA). FastQC was used to calculate the quality control statistics for the data generated by the Illumina HiSeq4000, and the resulting libraries were then subjected to paired-end sequencing (2 × 150bp).

To calculate the expression level of skin genes, salmon[13] software was utilized based on the whole-length transcripts of goat skin as a reference sequence. Then, differential expression genes(DEGs) were detected by EdgeR package of R [40]. We normalized the expression matrix of DEGs by dividing each value for a gene by the maximum value observed in any sample for that gene. To analyze the annual transcriptomes of goat skin, we used the MetaCycle[41], an integrated R package to evaluate periodicity in large scale data, to find the annual rhythm expressed genes.

Seasonal Skin sRNA sequencing

We collected 8 body side skin samples from three Inner Mongolia Cashmere Goats at eight-month (Jan, Apr, May, Jul, Aug, Sep, Oct, and Dec) and classified winter (Dec and Jan), spring (Apr and May), summer (Jul and Aug), fall (Sep and Oct). A total amount of 2.5 ng RNA per sample was used as input material for the RNA sample preparations. Sequencing libraries were generated using NEBNext® small RNA Sample Library Prep Kit for Illumina (NEB, USA) following the manufacturer's recommendations and index codes were added to attribute sequences to each sample. After cluster generation, the library preparations were sequenced on an Illumina Hiseq 2500 platform and paired-end reads were generated. miRDeep2 was utilized to detect mature miRNAs and predict novel miRNAs[42]. The differential expressed miRNAs (DEMs) were identified by the DESeq package in the R language[43].

Bio-information Analyses

To analyze the role of transcript factor in SRGs, we utilized the AnimalTFDB was used to investigate the regulator motifs in 5'FTR of SRGs. To classify the function of seasonal rhythm genes, ClueGO, a plugin of the Cytoscape platform[44], was used. Enrichment/Depletion (Two-sided hypergeometric test), Correction Method (Bonferroni step down), Min GO Level (3), Max GO Level (12), GO Fusion (false), GO Group (true) were settled. To analyze the rhythm of DEGs of goat skin, MetaCycle[41] was utilized. We tried from 4 months to one year as a length of interesting rhythms. And then to bridge the relationship between DEMs and SRGs, miRanda [45] was used to find the binding site in SRGs sequence for DEMs. Then, interaction networks of DEMs and SRGs was carrying out by the Cytoscape.

Declarations

Ethical Approval and Consent to participate

My manuscript report data collected from cashmere goat skin. The sampling procedure was according to the standards of the Animal Care and Use Committee in Inner Mongolia University for Nationalities, China.

Consent for publication

All authors provided consent for publication.

Availability of supporting data

The multiple Omics data used; analysis pipeline used in this study will be made available from the corresponding author upon request.

Competing interests

The authors declare that there are no competing interests.

Funding

This work was supported by the Doctoral Scientific Research Foundation of Inner Mongolia University for Nationalities (BS527) to Dr. Jianghong Wu, the National Natural Science

Foundation of China (31560623) to Dr. Jianghong Wu, the Innovation Foundation of IMAAAHS (2017CXJJM03-2) Dr. Jianghong Wu, and the Natural Science Foundation of Inner Mongolian (2018MS03034) to Dr. Jianghong Wu. The authors declare that the grant, scholarship and/or funding for this study do not lead to any conflict of interest. The funders had no role in study design, data collection and analysis, decision to publish, or preparation of the manuscript.

Authors' contributions

Conceived and designed the experiments: JW. Performed the experiments: JW YL HS. Analyzed the data: HG JW. Contributed reagents/materials/ analysis tools: YL DW CL. Wrote the paper: JW.

Authors' information

Jianghong Wu (wujianghonglong@126.com, College of Animal Science and Technology, Inner Mongolia University for Nationalities, Tongliao, 028000, China; Inner Mongolia Academy of Agricultural & Animal Husbandry Sciences, Hohhot, 010031, China)

Yin li (79588471@qq.com, College of Animal Science and Technology, Inner Mongolia University for Nationalities, Tongliao, 028000, China)

Husile Gong (huslee@163.com, College of Life Science, Inner Mongolia University for Nationalities, Tongliao, 028000, China)

Dubala Wu (yinghua19870901@163.com, College of Animal Science and Technology, Inner Mongolia University for Nationalities, Tongliao, 028000, China)

Chun Li (lichun1985@126.com, College of Animal Science and Technology, Inner Mongolia University for Nationalities, Tongliao, 028000, China)

Bin Liu (liubin0613@126.com, Inner Mongolia Academy of Agricultural & Animal Husbandry Sciences, Hohhot, 010031, China)

References

1. Dopico, X.C., et al., *Widespread seasonal gene expression reveals annual differences in human immunity and physiology.* Nat Commun, 2015. **6**: p. 7000.
2. Dekens, M.P., et al., *Light regulates the cell cycle in zebrafish.* Curr Biol, 2003. **13**(23): p. 2051-7.
3. Vallone, D., et al., *E-box function in a period gene repressed by light.* Proc Natl Acad Sci U S A, 2004. **101**(12): p. 4106-11.
4. Walter, R.B., et al., *Exposure to fluorescent light triggers down regulation of genes involved with mitotic progression in Xiphophorus skin.* Comp Biochem Physiol C Toxicol Pharmacol, 2015. **178**: p. 93-103.
5. Yufera, M., et al., *The circadian transcriptome of marine fish (Sparus aurata) larvae reveals highly synchronized biological processes at the whole organism level.* Sci Rep, 2017. **7**(1): p. 12943.
6. Tanioka, M., et al., *Molecular clocks in mouse skin.* J Invest Dermatol, 2009. **129**(5): p. 1225-31.
7. Sandu, C., et al., *Circadian clocks in rat skin and dermal fibroblasts: differential effects of aging, temperature and melatonin*. Cell Mol Life Sci, 2015. **72**(11): p. 2237-48.

8. Balsalobre, A., F. Damiola, and U. Schibler, *A serum shock induces circadian gene expression in mammalian tissue culture cells.* Cell, 1998. **93**(6): p. 929-37.
9. Sporl, F., et al., *A circadian clock in HaCaT keratinocytes.* J Invest Dermatol, 2011. **131**(2): p. 338-48.
10. Shin, S.Y., et al., *Agerarin, identified from Ageratum houstonianum, stimulates circadian CLOCK-mediated aquaporin-3 gene expression in HaCaT keratinocytes.* Sci Rep, 2017. **7**(1): p. 11175.
11. Nagoshi, E., et al., *Circadian gene expression in individual fibroblasts: cell-autonomous and self-sustained oscillators pass time to daughter cells.* Cell, 2004. **119**(5): p. 693-705.
12. Sandu, C., et al., *Human skin keratinocytes, melanocytes, and fibroblasts contain distinct circadian clock machineries.* Cell Mol Life Sci, 2012. **69**(19): p. 3329-39.
13. Patro, R., et al., *Salmon provides fast and bias-aware quantification of transcript expression.* Nat Methods, 2017. **14**(4): p. 417-419.
14. Xiong, T.F., F.Q. Pan, and D. Li, *Expression and clinical significance of S100 family genes in patients with melanoma.* Melanoma Res, 2019. **29**(1): p. 23-29.
15. Zhou, W., et al., *MiR-206-mediated dynamic mechanism of the mammalian circadian clock.* BMC Syst Biol, 2011. **5**: p. 141.
16. Ko, C.H. and J.S. Takahashi, *Molecular components of the mammalian circadian clock.* Hum Mol Genet, 2006. **15 Spec No 2**: p. R271-7.
17. Schneider, M.J., et al., *Targeted disruption of the type 1 selenodeiodinase gene (Dio1) results in marked changes in thyroid hormone economy in mice.* Endocrinology, 2006. **147**(1): p. 580-9.
18. Schweizer, U., J.M. Weitzel, and L. Schomburg, *Think globally: Act locally : New insights into the local regulation of thyroid hormone availability challenge long accepted dogmas.* Molecular & Cellular Endocrinology, 2008. **289**(1): p. 1-9.
19. Billoni, N., et al., *Thyroid hormone receptor beta1 is expressed in the human hair follicle.* Br J Dermatol, 2000. **142**(4): p. 645-52.
20. Winter, H., et al., *Thyroid hormone receptor alpha1 is a critical regulator for the expression of ion channels during final differentiation of outer hair cells.* Histochem Cell Biol, 2007. **128**(1): p. 65-75.
21. Dettling, J., et al., *Autonomous functions of murine thyroid hormone receptor TRalpha and TRbeta in cochlear hair cells.* Mol Cell Endocrinol, 2014. **382**(1): p. 26-37.
22. Wood, S.H., et al., *Binary Switching of Calendar Cells in the Pituitary Defines the Phase of the Circannual Cycle in Mammals.* Curr Biol, 2015. **25**(20): p. 2651-62.
23. Schey, K.L., et al., *Aquaporins in the eye: expression, function, and roles in ocular disease.* Biochim Biophys Acta, 2014. **1840**(5): p. 1513-23.
24. van Genderen, M.M., et al., *Mutations in TRPM1 are a common cause of complete congenital stationary night blindness.* Am J Hum Genet, 2009. **85**(5): p. 730-6.
25. Su, M., et al., *Role of the p53TRPM1/miR211MMP9 axis in UVBinduced human melanocyte migration and its potential in repigmentation.* Int J Mol Med, 2020. **45**(4): p. 1017-1026.
26. Barbato, S., et al., *MiR-211 is essential for adult cone photoreceptor maintenance and visual function.* Sci Rep, 2017. **7**(1).
27. Kozlyuk, N., et al., *S100 Proteins in the Innate Immune Response to Pathogens.* Methods Mol Biol, 2019. **1929**: p. 275-290.

28. Alowami, S., et al., *Psoriasin (S100A7) expression is altered during skin tumorigenesis.* BMC dermatology, 2003. **3**(1): p. 1.
29. Moubayed, N., et al., *Psoriasin (S100A7) is significantly up-regulated in human epithelial skin tumours.* Journal of cancer research and clinical oncology, 2007. **133**(4): p. 253-261.
30. Jayakanthan, K., et al., *High expression of S100 calgranulins genes in peripheral blood mononuclear cells in patients with Takayasu arteritis.* Cytokine, 2018. **114**: p. 61-66.
31. Gong, H., et al., *Evolution and Expression of S100A7 Gene in Vertebrates.* Biochem Genet, 2018.
32. Glaser, R., et al., *UV-B radiation induces the expression of antimicrobial peptides in human keratinocytes in vitro and in vivo.* J Allergy Clin Immunol, 2009. **123**(5): p. 1117-23.
33. Son, E.D., et al., *S100A7 (psoriasin) inhibits human epidermal differentiation by enhanced IL-6 secretion through IκB/NF-κB signaling*. Experimental Dermatology, 2016. **25**(8): p. 636-641.
34. Zhou, G., et al., *Reciprocal negative regulation between S100A7/psoriasin and β-catenin signaling plays an important role in tumor progression of squamous cell carcinoma of oral cavity.* Oncogene, 2008. **27**(25): p. 3527-3538.
35. Mh, V.D.B., et al., *Induction of Canonical Wnt Signaling by the Alarmins S100A8/A9 in Murine Knee Joints: Implications for Osteoarthritis.* Arthritis & Rheumatology, 2016. **68**(1): p. 152-163.
36. Contreras-Jurado, C., et al., *Impaired hair growth and wound healing in mice lacking thyroid hormone receptors*. PLoS One, 2014. **9**(9): p. e108137.
37. Ruiz-Llorente, L., et al., *Thyroid Hormone Receptors Regulate the Expression of microRNAs with Key Roles in Skin Homeostasis.* Thyroid, 2018. **28**(7): p. 921-932.
38. Garcia-Serrano, L., et al., *The thyroid hormone receptors modulate the skin response to retinoids.* PLoS One, 2011. **6**(8): p. e23825.
39. Barakat-Walter, I., . *Role of thyroid hormones and their receptors in peripheral nerve regeneration.* Journal of Neurobiology, 2015. **40**(4): p. 541-559.
40. Nikolayeva, O. and M.D. Robinson, *edgeR for differential RNA-seq and ChIP-seq analysis: an application to stem cell biology.* Methods Mol Biol, 2014. **1150**: p. 45-79.
41. Wu, G., et al., *MetaCycle: an integrated R package to evaluate periodicity in large scale data.* Bioinformatics, 2016. **32**(21): p. 3351-3353.
42. Mackowiak, S.D., *Identification of novel and known miRNAs in deep-sequencing data with miRDeep2.* Curr Protoc Bioinformatics, 2011. **Chapter 12**: p. Unit 12 10.
43. Anders, S. and W. Huber, *Differential expression analysis for sequence count data.* Genome Biol, 2010. **11**(10): p. R106.
44. Bindea, G., et al., *ClueGO: a Cytoscape plug-in to decipher functionally grouped gene ontology and pathway annotation networks.* Bioinformatics, 2009. **25**(8): p. 1091-3.
45. Betel, D., et al., *The microRNA.org resource: targets and expression.* Nucleic Acids Res, 2008. **36**(Database issue): p. D149-53.

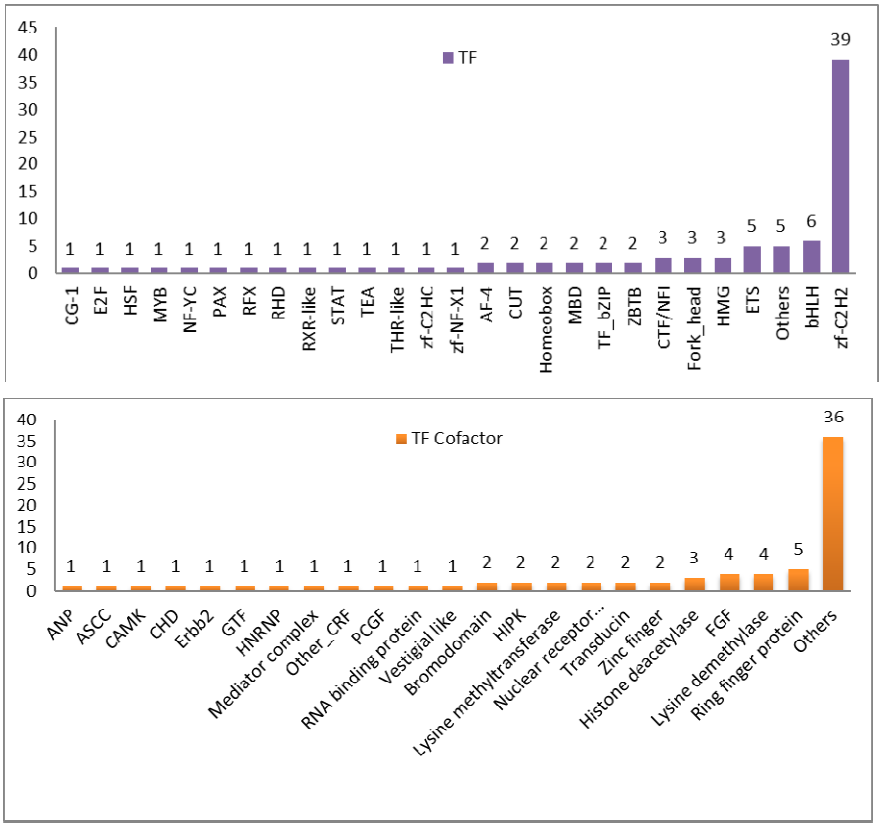

Supplement file 1 the class of transcript factor (top) and TF cofactor(bottom) for SRGs

Supplement file 2 the information of differential expressed miRNAs between summer and winter.

DEMs ID	Similar seed	Sequence	Summer	Winter	FC	pval	padj
NW_017189517.1_30891*	ggo-miR-1298	TTCATTCGGCTGTCCAGATGTA	23.9	179.9	0.133	0.000	0.000
chi-miR-206		TGGAATGTAAGGAAGTGTGTGGT	292.6	1126.2	0.260	0.002	0.098
NC_030818.1_13884#	bmo-miR-3357	TCTGGTCTCGGAAGCTAAGCAGGG	3070.2	971.8	3.159	0.002	0.090
NC_030817.1_12559#	sma-miR-8445-3p	CAGGTAGGAATAATGGAAT	1020.4	302.3	3.376	0.002	0.080
NC_030811.1_5473#	eca-miR-9152	ACCGGGTGCCGTAGGCTT	114064.6	33310.4	3.424	0.002	0.080
NC_030823.1_18736#	mmu-miR-678	ATCTCGGTGGGGCCTCCA	1311.1	378.5	3.464	0.001	0.071
NC_030808.1_1154#	pab-miR11409d	AATTTGACTGGCTTTTAT	160.2	45.9	3.490	0.002	0.075
chi-miR-144-5p		TGGGATATCATCATATACTGT	1442.2	390.4	3.694	0.000	0.025
NW_017212547.1_31955#	hsa-miR-214-5p	CGCCTGTCTGCGCGTCGCT	33832.7	8671.4	3.902	0.000	0.025

NC_030818.1_14129#	rno-miR-3583-5p	CGCATGAATGGATGAACGGG	632.2	159.5	3.964	0.001	0.043
NC_030817.1_12367#	dre-miR-92b-5p	TGGTGTGGAGCCGGGCGTGGA	548.6	137.8	3.982	0.001	0.036
NC_030821.1_16866#	pal-miR-541-3p	CGGGCGCATTTCCACCACGGC	246.0	61.3	4.010	0.001	0.042
NC_030810.1_4400#	ppy-miR-613	GGGGATGTGGCTCAGTGG	348.5	86.2	4.043	0.001	0.042
NC_030810.1_4496#	eca-miR-9152	ACCGGGTGCTGTGGGCCA	156.6	38.2	4.098	0.002	0.080
NC_030819.1_15003#	hsa-miR-3162-5p	TTAGGGAGGACAGAAACCT	165.9	39.6	4.193	0.001	0.052
NC_030827.1_23154#	hsa-miR-4421	GCCTGTCTGAGCGTCCCT	4534.8	1040.8	4.357	0.000	0.017
NC_030826.1_21385#-	-	GAGCAGTAACAGGTCTGT	305.5	69.9	4.370	0.001	0.042
NC_030826.1_22781#	mmu-miR-3062-3p	CGGGGACAGTGCCAGGTAGG	193.7	43.8	4.424	0.001	0.060
NC_030828.1_23548#	mdo-miR-12332-3p	TTCCCGGCCAGTGCACCA	2553.6	566.5	4.508	0.000	0.011
NC_030811.1_5498#	osa-miR5791	CTGCAGGACGGTGGCCATG	198.9	44.0	4.520	0.001	0.048
NC_030822.1_17540#	str-miR-9-3p	AAAGCTGAAACTTAGAGGA	286.0	63.0	4.543	0.000	0.020
chi-miR-451-5p		AAACCGTTACCATTACTGA	90218.0	19545.6	4.616	0.000	0.009
NC_030834.1_28382*	cfa-miR-486	TCCTGTACTGAGCTGCCCCGAGG	32104.1	6943.7	4.623	0.000	0.009
NC_030829.1_24372#	cli-miR-1791-3p	AGATGTGATTTCTGCCCA	261.9	56.5	4.632	0.000	0.021
NC_030826.1_21983#	esi-miR3454a-5p	ATCCCAGCGGTGCCTCCG	517.2	110.4	4.683	0.000	0.018
NC_030826.1_21706#	bta-miR-320b	GGCTGGGTCGGTCGGGCA	263.7	55.8	4.723	0.000	0.025
NC_030826.1_22790#	hsa-miR-4467	CGGCGGCGGCGGCTCTGGACG	1299.4	268.8	4.834	0.000	0.009
NC_030816.1_11778#	mdo-miR-12332-3p	TTCCCGGCCAATGTACCT	165.1	34.1	4.837	0.000	0.025
chi-miR-211		TTCCCTTTGTCATCCTTTGCCC	1534.1	312.1	4.916	0.000	0.007
chi-miR-144-3p		TACAGTATAGATGATGTAC	226.7	44.0	5.156	0.000	0.011
NC_030811.1_5300#	bta-miR-2299-3p	CCCGGGGAGGTAGTGACT	129.0	25.0	5.167	0.000	0.025
NC_030818.1_13661#	hsa-miR-887-5p	CTTGGGAGCGGGCGGGCGGC	94.6	18.3	5.173	0.001	0.042
NC_030813.1_8487#	cel-miR-2208b-3p	GTGCAGATCTTGGTGGCA	114.8	20.6	5.570	0.001	0.036
NC_030824.1_19166#	dvi-miR-9701b-5p	TGGTGAACTATGCCTGGAA	111.7	19.8	5.632	0.000	0.031
NC_030809.1_2123#	cpo-miR-12084-3p	CCGCGGCTGGACGAGGCA	201.0	32.6	6.172	0.000	0.010

Note. # represents the miRNAs were novel miRNA and * for the miRNAs have the similar seed with the mature miRNAs in miRbase.